Received: 1 September 2021 | Revised: 13 September 2021 | Accepted: 17 September 2021

DOI: 10.1002/jcla.24032

RESEARCH ARTICLE

WILEY

miR-3146 induces neutrophil extracellular traps to aggravate gout flare

Lizhen Shan[1] | Di Yang[2] | Fabo Feng[2] | Danjie Zhu[2] | Xiaolin Li[2]

[1]Department of Endocrinology and Metabolism, The Second Affiliated Hospital, Zhejiang University School of Medicine, Hangzhou, China

[2]Department of Orthopaedic Surgery, Zhejiang Provincial People's Hospital, People's Hospital of Hangzhou Medical College, Hangzhou, China

Correspondence
Di Yang, Department of Orthopaedic Surgery, Zhejiang Provincial People's Hospital, People's Hospital of Hangzhou Medical College, Shangtang Road 158, Hangzhou 310014, Zhejiang, China.
Email: yangdi@hmc.edu.cn

Funding information
This study was supported by Natural Science Foundation of Zhejiang Province (LY18H060009), Medical Health Science and Technology Project of Zhejiang Provincial Health Commission (2019KY019),the Natural Science Foundation of Zhejiang Province(LQ19H160014) and Medical Health Science and Technology Project of Zhejiang Provincial Health Commission(2019KY320)

Abstract

Background: Gout is an inflammatory arthritis and is characterized by the accumulation of deposited monosodium urate (MSU) crystals in the joints. miRNAs may act as key regulators of gout pathogenesis. The aim of our study was to explore the underlying role and molecular mechanism of miR-3146 in the formation of neutrophil extracellular traps (NETs) during the pathogenesis of gout.

Methods: The expression of miR-3146 and sirtuin 1 (SIRT1) was determined by real-time reverse transcription-polymerase chain reaction and Western blot, respectively. The luciferase reporter assay was performed to identify the targeting relationship between miR-3146 and SIRT1. Reactive oxygen species (ROS) production was detected by fluorescent staining. NETs formation was demonstrated via immunofluorescence staining and ELISA method. Gout model was induced in rats to verify the effects of miR-3146 inhibition on histopathological changes and NETs.

Results: Here, we found miR-3146 expression was dramatically increased in neutrophils of patients with gout, which was accompanied with the higher levels of NETs. MSU crystals significantly increased miR-3146 expression and ROS production in neutrophils. The NETs process was also triggered by MSU crystals. Furthermore, we verified the interaction between miR-3146 and SIRT1. Additionally, antagomir-3146-based therapy effectively inhibited the formation of NETs in rats with gout.

Conclusion: Our findings indicated that miR-3146-mediated NETs formation may play a potential role in the pathogenesis of gout. These results suggested that miR-3146 could be used as a potential therapeutic target for the treatment of gout.

KEYWORDS
gout, miR-3146, neutrophil extracellular traps, oxidative stress, SIRT1

1 | INTRODUCTION

Gout is a heterogeneous disease characterized by chronic hyperuricemia resulting from the deposition of monosodium urate (MSU) crystals in joints, kidneys, and other soft tissues.[1] Gout flare is a common rheumatic disease featured with inflammatory cell infiltration, joint swelling and severe pain.[2] However, due to the self-limited nature and short course, patients with gout during gout flare often fail to receive conventional urate-lowering therapy after pain relief, resulting in repeated attacks of arthritis. Therefore, the effective therapeutic strategies of gout flare based on the underlying mechanism of bone destruction caused by MSU crystals are current research hotspot.

With the deepening of research, the discovery of neutrophil extracellular traps (NETs) and oxidative stress opens a new perspective to understand the role of neutrophils in the pathogenesis of gout. NETosis is a form of neutrophil death that is distinguished from apoptosis or necrosis in response to pathogens or other irritants.[3] NETs are extracellular structures with various biological activities, which are released by apoptotic neutrophils.[4] In the course of gout, the formation of early NETs increases the inflammatory response. The rapid chemotaxis of neutrophils to inflammatory sites to aggregate NETs (aggNETs), leading to the degradation of inflammatory cytokines through a variety of hydrolases, indicating that NETosis is involved in the pathogenesis of gout.[5] Oxidative stress is an early event of gout that can damage different biomolecules, inhibit hyperblastosis, and cause cell membrane destruction and cell death and refers to elevated reactive oxygen species (ROS) levels.[6] It has been previously shown that the induction of NETosis depends on ROS, the main source of which is NADPH oxidase.[7,8]

miRNAs are non-coding small RNAs containing endogenous 21–23 nucleotides, which are involved in the regulation of eukaryotic gene expression via post-transcriptional levels by binding to 3′-UTR of mRNA of their target genes.[9] Recently, a number of miRNAs have been implicated in inflammatory arthritis, including gout and have been identified as significant biomarkers for the diagnosis and treatment of gout.[10,11] Liu et al reported that the expression of miR-3146 was upregulated in the plasma of gout patients compared with asymptomatic hyperuricemia group.[12] However, there is no evidence to support that miR-3146 is involved in MSU crystals-induced NETosis. Herein, we mainly explored the functional role of miR-3146 in the pathogenesis of gout.

2 | MATERIALS AND METHODS

2.1 | Patients

We recruited a total of 30 male patients with gout during gout flare (ranges from 30 to 65 years) according to the 2011 recommendations for the diagnosis and management of gout and hyperuricemia,[13] from January 2020 to December 2020 in Zhejiang Provincial People's Hospital. Exclusion criteria were: declining to participate in the study; suffering from another clinical condition that causes hyperuricemia or cytokine production, such as hemolytic anemia, myeloproliferative disorders, psoriasis, sarcoidosis, acute or chronic renal failure, alcohol intoxication, diabetic ketoacidosis, lactic acidosis, glycogen storage disease type I, hypo- or hyperparathyroidism, or concurrent infections. In addition, 30 healthy volunteers (ranges from 27 to 60 years) who underwent physical examinations during the same period were enrolled as controls. There were no significant difference in age and distribution of gender between gout and healthy group. Blood samples were collected from each participant. All experimental protocols were approved by the Ethics Committee of Zhejiang Provincial People's Hospital (Approval number: 2020QT119), and informed consent was obtained from all patients and control subjects. Whole blood was collected from each subject using heparin anticoagulant tube, centrifuged at 1500 *g* for 10 min at 4°C and the plasma thus obtained was frozen at −80°C for the following experiments.

2.2 | Cell isolation and culture

Neutrophil fraction was separated from fresh peripheral blood of all patients with gout and the healthy subjects using density gradient centrifugation as previously described.[14] Neutrophils were isolated from heparinized blood using commercially available kit (EasySep Human Neutrophil Enrichment Kit, STEMCELL Technologies Inc.). Briefly, a standard procedure of Histopaque-1077 (Sigma-Aldrich Chemical Co) gradient density centrifugation was used to separate polymorphonuclear leukocytes (PMNs) from mononuclear cells (PBMCs). After centrifugation, the layer of plasma and mononuclear cells was discarded and the remaining erythrocytes/granulocytes were transferred into a fresh tube for erythrocytes lysis with a hypotonic ammonium chloride solution. Obtained PMNs were used for the isolation of neutrophils according to neutrophil enrichment kit protocol provided by the manufacturer. The isolated neutrophils were maintained in RPMI-1640 medium (Gibco) supplemented with 10% heat-inactivated fetal bovine serum, 100 U/ml penicillin and 100 μg/ml streptomycin. Neutrophils (1×10^7 cells/ml) obtained from healthy subjects were transfected with miR-3146 mimic, inhibitor, or negative controls or stimulated with 1 mg/ml MSU crystals (Sigma-Aldrich) for 2 h after treatment with or without 10 mM ROS scavenger *N*-acetyl-L cysteine (NAC; Sigma-Aldrich) for 1 h.

2.3 | In-vivo assay

Adult male Sprague-Dawley rats (160–180 g), obtained from Center for Animal Experiment of Zhejiang University School of Medicine were used in this study. The rat model of gout was established via administration of 200 μl MSU (20 mg/ml) into the ankle joint cavity. Antagomir-3146 (10 μl) or an equal amount of normal saline was injected at the day of modeling. The animal procedures were approved by the Institutional Animal Care and Use Committee of Zhejiang University School of Medicine (Approval number: 2019-032). The synovial tissue specimens were removed from the left knee.

FIGURE 1 miR-3146 is significantly upregulated in patients with gout. The expression of miR-3146 in patients with gout and healthy volunteers (A); NETs formation was assessed by circulating MPO-DNA capture ELISA method (B) and representative immunofluorescence staining of Ly6G (scale bars show 25-mm intervals; magnification ×40) (C); The ROS production (D), the mRNA and protein levels of SIRT1 (E, F) and the serum levels of IL-8 and IL-1β (G) were determined. Data from at least three independent experiments were expressed as mean ± SD. $^{**}p < 0.01$ versus healthy group

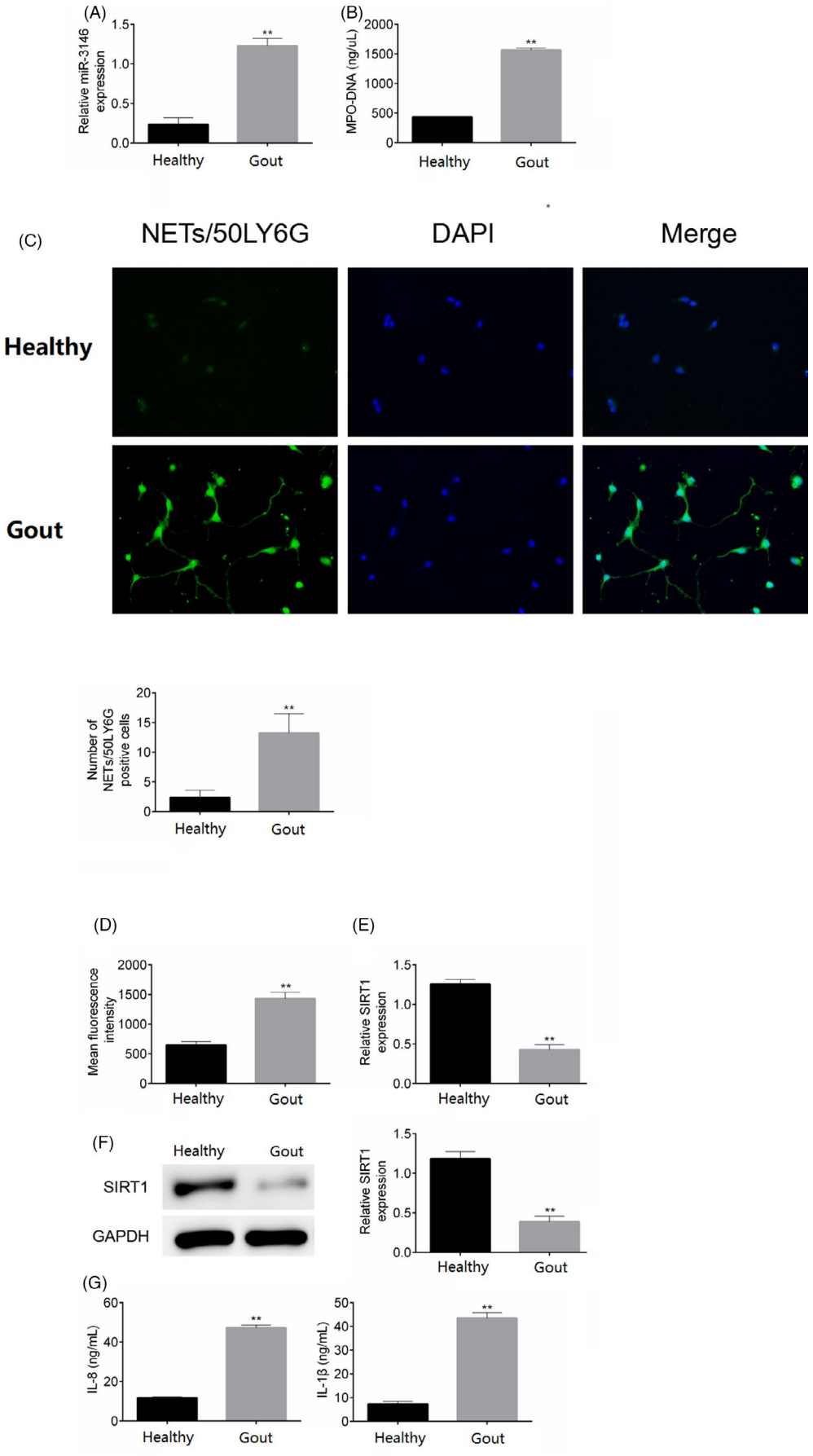
(A)
Relative miR-3146 expression
1.5
1.0
0.5
0.0
**
Healthy
Gout
(B)
MPO-DNA (ng/uL)
2000
1500
1000
500
0
**
Healthy
Gout
(C)
NETs/50LY6G
DAPI
Merge
Healthy
Gout
Number of NETs/50LY6G positive cells
20
15
10
5
0
**
Healthy
Gout
(D)
Mean fluorescence intensity
2000
1500
1000
500
0
**
Healthy
Gout
(E)
Relative SIRT1 expression
1.5
1.0
0.5
0.0
**
Healthy
Gout
(F)
Healthy
Gout
SIRT1
GAPDH
Relative SIRT1 expression
1.5
1.0
0.5
0.0
**
Healthy
Gout
(G)
IL-8 (ng/mL)
60
40
20
0
**
Healthy
Gout
IL-1β (ng/mL)
50
40
30
20
10
0
**
Healthy
Gout

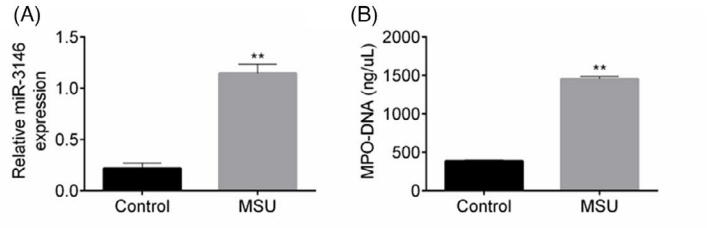
(A)
Relative miR-3146 expression
1.5
1.0
0.5
0.0
**
Control
MSU
(B)
MPO-DNA (ng/uL)
2000
1500
1000
500
0
**
Control
MSU

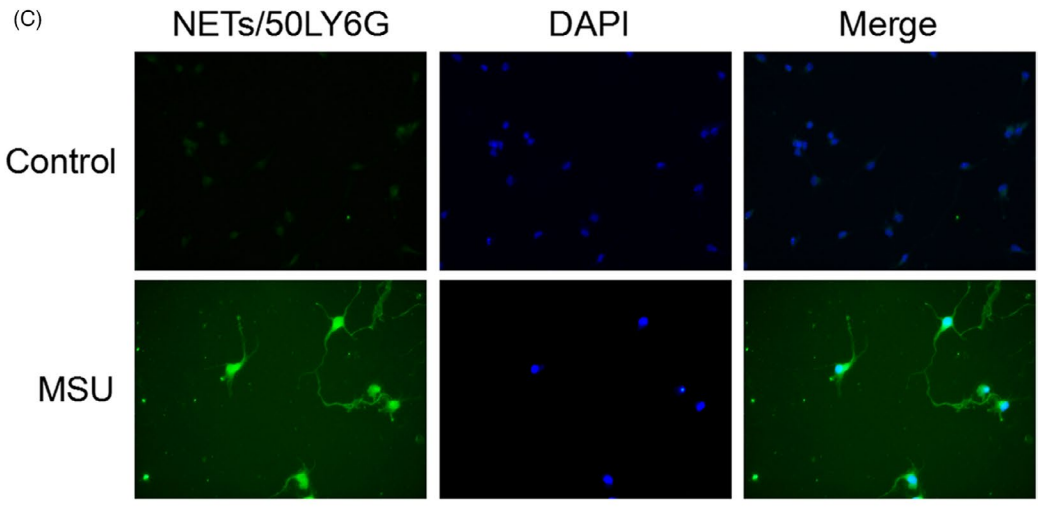
(C)
NETs/50LY6G
DAPI
Merge
Control
MSU

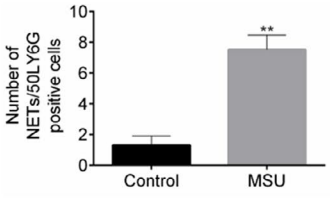
Number of NETs/50LY6G positive cells
10
8
6
4
2
0
**
Control
MSU

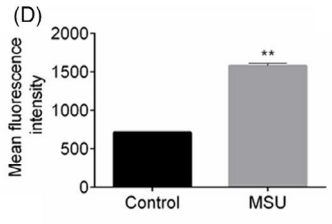
(D)
Mean fluorescence intensity
2000
1500
1000
500
0
**
Control
MSU

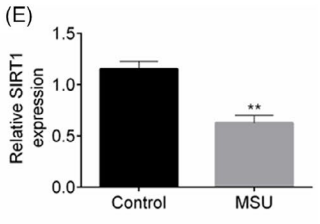
(E)
Relative SIRT1 expression
1.5
1.0
0.5
0.0
**
Control
MSU

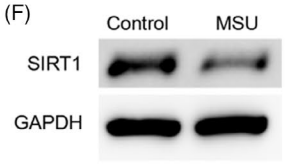
(F)
Control
MSU
SIRT1
GAPDH

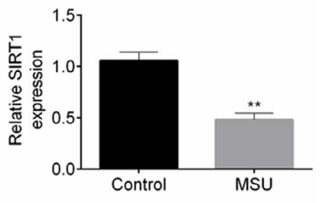
Relative SIRT1 expression
1.5
1.0
0.5
0.0
**
Control
MSU

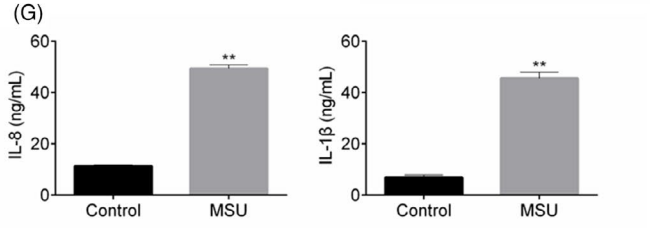
(G)
IL-8 (ng/mL)
60
40
20
0
**
Control
MSU
IL-1β (ng/mL)
60
40
20
0
**
Control
MSU

FIGURE 2 Neutrophil miR-3146 and ROS production are increased in response to MSU crystals. The expression of miR-3146 (A), NETs formation (B, C), ROS production (D), the mRNA and protein levels of SIRT1 (E, F) and the levels of IL-8 and IL-1β (G) in human neutrophils stimulated with or without MSU crystals. Data from at least three independent experiments ($n = 3$) were expressed as mean ± SD. $^{**}p < 0.01$ versus control group

2.4 | Histopathological examination

The synovial tissues were fixed in 10% paraformaldehyde overnight before decalcification using ethanol and processed for paraffin embedding. Tissue sections (5 μm) were stained with hematoxylin and eosin. Before staining, slides were deparaffinized. To investigate morphologic changes, sections were stained with hematoxylin (Merck) and 1% eosin (Sigma-Aldrich), air-dried, and cover-slipped. All slides (×100 magnification) were observed and photographed using a microscope equipped with camera (BX51; Olympus Ltd.), and images were analyzed using DP2-BSW software (Olympus Ltd).

2.5 | Measurement of oxidative indicators

The indicators of oxidative damage (MDA, SOD and GSH-Px) were measured using the commercial kits (Beijing Boaosen Biotechnology, Ltd.) following the manufacturer's protocols.

2.6 | Luciferase reporter assay

The putative binding sites of miR-3146 in the 3′-UTR of the human sirtuin 1 (SIRT1) gene transcript were predicted by TargetScan (http://www.targetscan.org/), and then verified by luciferase reporter gene assay. HEK-293 cells purchased from the American Type Culture Collection (ATCC) were cultured in DMEM supplemented with 10% FBS and 100 μg/ml penicillin/streptomycin (all from Gibco) at 37°C with 5% CO_2.

According to the manufacturer's instructions, luciferase assays were performed in HEK-293 cells after co-transfection with the wild/mutated types of SIRT1 promoter reporters and miR-3146 mimic/mimic NC using Lipofectamine 2000. After 48 h, the cells were collected and tested for luciferase activities using the dual-luciferase reporter assay system (Promega).

2.7 | RNA extraction and quantitative real-time PCR

Total RNA was extracted from cells using TRIzol (Invitrogen) and converted into cDNA using the PrimeScript RT reagent kit (Takara) according to the manufacturer's instructions. The relative expression levels of miR-3146 and SIRT1 were measured by real-time PCR using SYBR Green I real-time PCR kit (BD Biosciences) on an ABI 7500 Real-Time PCR system (Applied Biosystems). The cycling conditions were as follows: initial denaturation at 95°C for 15 s, followed by 45 cycles of 55°C for 33 s and 70°C for

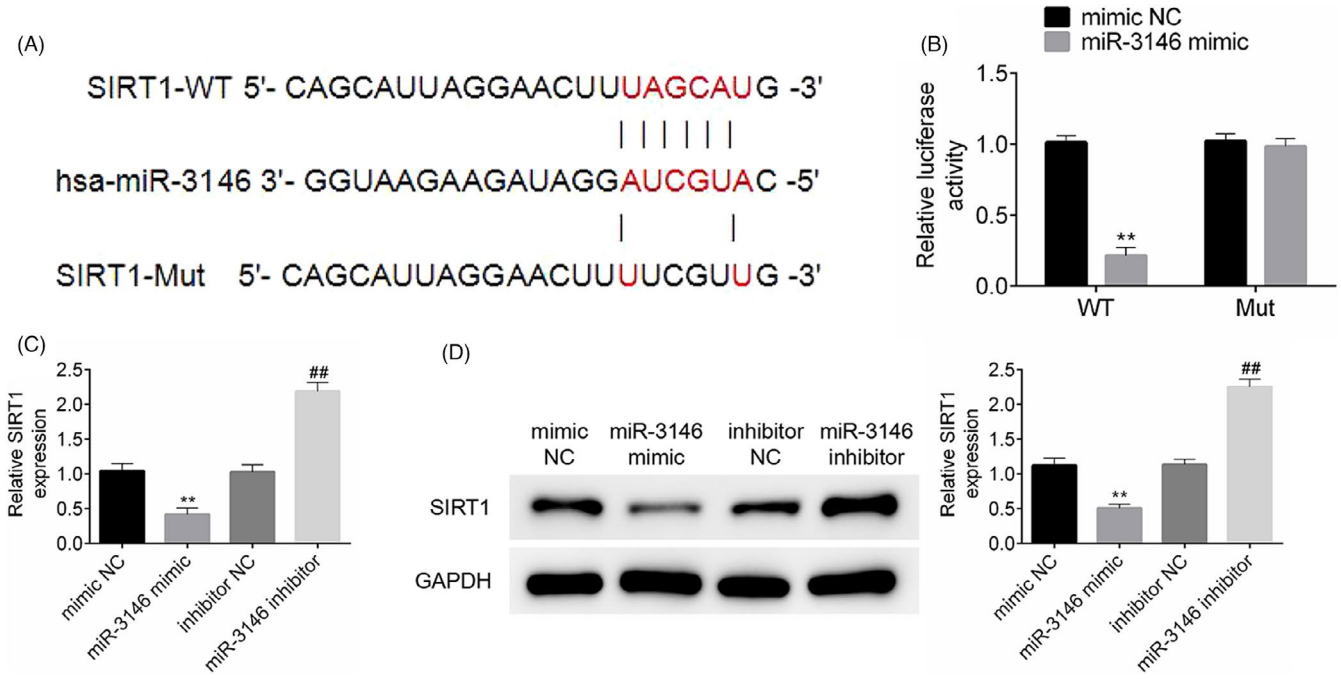

FIGURE 3 miR-3146 directly targets SIRT1 in neutrophils. SIRT1 mRNA 3′UTR contained miR-3146 binding sites predicted by TargetScan (A); The luciferase activities were measured in human neutrophils transfected with the wild or mutant type SIRT1 plasmids (B). The mRNA and protein levels of SIRT1 were measured in human neutrophils transfected with miR-3146 mimic or inhibitor (C, D). Data from at least three independent experiments ($n = 3$) were expressed as mean ± SD. $^{**}p < 0.01$ versus mimic NC group; $^{\#\#}p < 0.01$ versus inhibitor NC group

30 s. The relative expressions were calculated through the $2^{-\Delta\Delta Ct}$ method. U6 and GAPDH were used as internal controls, respectively. The primers used were as follows: miR-3146, forward: 5′-CATGCTAGGATAGAAAGAATGG-3′, reverse: universal primers; SIRT1, forward: 5′-TAGCCTTGTCAGATAAGGAAGGA-3′, reverse 5′-ACAGCTTCACAGTCAACTTTGT-3′; U6, forward: 5′-AAAGCAAATCATCGGACGACC-3′, reverse 5′-GTACAACACATTGTTTCCTCGGA-3′; GAPDH, forward: 5′-TGTGGGCATCAATGGATTTGG-3′, reverse 5′-ACACCATGTATTCCGGGTCAAT-3′.

2.8 | Western blot

Total proteins were extracted from cultured cells using radioimmunoprecipitation buffer (RIPA). Equal amount of denatured protein samples were separated by electrophoresis and transferred to polyvinylidene fluoride membranes. Immunoblotting was performed at 4°C overnight with appropriate primary antibodies against SIRT1 (#9475; Cell Signaling Technology) at a dilution of 1:1000. After incubating with HRP-conjugated secondary antibodies (#7074; 1:2000 dilution, Cell Signaling Technology), the signals were visualized by the ECL system (Thermo Fisher Scientific). β-actin was used as a loading control.

2.9 | Enzyme-linked immunosorbent assay

IL-8 and IL-1β concentrations in cell culture supernates and serum were quantified using commercial enzyme-linked immunosorbent assay (ELISA) kits (human IL-8 and IL-1β ELISA reagent kits from R&D Systems; rat IL-8 and IL-1β ELISA reagent kits from R&D Systems and Shanghai Enzyme-linked Biotechnology Co., Ltd.), following the manufacturer's instructions. The microplates were sensitized overnight with coating antibody and blocked with a solution of 4% serine bovine albumin, 5% sucrose in PBS. Supernatants and serum samples and standards were placed in duplicate in the wells of the plate and incubated at 37°C for 1 h. Samples were washed and detection antibody was added and incubated for 1 h. After appropriate washings, streptavidin conjugated to horseradish peroxidase was added and incubation was performed at 37°C for 30 min. The reaction was evidenced by the addition of TMB, which was incubated for 10 min at 37°C. The reaction was stopped with H_2SO_4 and read at 450 nm in an ELISA reader (Microplate Reader, SPECTROstarNano, BGM/LABTECH).

For myeloperoxidase (MPO)-DNA complex ELISA assay as previously described,[15] a "sandwich" ELISA with anti-MPO monoclonal antibody (Merck Millipore Corp., catalog no. 07–496) and peroxidase-conjugated anti-DNA monoclonal antibody (Roche Diagnostics; Cell Death Detection ELISA no. 1154467500) was used. Briefly, the wells of microtiter strips were coated with a monoclonal antibody specific for MPO to capture MPO-DNA derived from NETs. A peroxidase substrate was added, which reacted with the bound peroxidase to yield a soluble green product detected at 405 nm. Absorbance readings were proportional to the amount of bound horseradish peroxidase-labeled anti-DNA monoclonal antibody. Results were expressed in arbitrary units.

2.10 | Immunofluorescence staining

Synovial tissues were digested in Hank's Balanced Salt Solution (Thermo Fisher Scientific) containing 0.25% trypsin (Gibco) at 37°C. Treated neutrophils or embedded tissues were fixed in 4% paraformaldehyde for 15 min and permeabilized in 0.01% Triton X-100 for 10 min at room temperature. Samples were then stained with citrullinated histone H3 (CitH3) (1:50 dilution; Abcam) and LYG6 antibodies (1:100 dilution; eBioscience). The nucleus was counter-stained with DAPI. Images were captured by confocal microscopy (Zeiss) from five randomly fields. The results were expressed as the number of NETs/50 Ly6G-positive cells.

2.11 | Measurement of intracellular ROS

Intracellular ROS accumulation was measured using dichlorofluorescin diacetate (DCFH-DA; Sigma-Aldrich) as a peroxide-sensitive fluorescent probe at the wavelength 488/525 nm as previously described.[16,17] Briefly, DCFH-DA was diluted in serum-free DMEM to a final concentration of 10 μM and was added to each well for replacing of original medium. After incubation for 30 min at 37°C, cells were washed thrice with serum-free DMEM. The fluorescence intensities were recorded with a spectrophotometer (Shimadzu Corporation) with an excitation of 485 nm and an emission of 525 nm.

2.12 | Statistical analysis

Data from at least three independent experiments were expressed as mean ± standard deviation (SD), analyzed by SPSS 19.0 statistical software (SPSS). One-way ANOVA was used to analyze the differences between groups. $p < 0.05$ indicated a statistically significant difference.

3 | RESULTS

3.1 | miR-3146 is significantly upregulated in patients with gout

As shown in Figure 1A, the expression of neutrophil miR-3146 was markedly upregulated in patients with gout relative to healthy volunteers. NETs formation, which was assessed by circulating MPO-DNA capture ELISA method (Figure 1B) and immunofluorescence microscopy (Figure 1C), was significantly increased in gout cases than that in the healthy controls, indicating that NETosis might be involved in the pathogenesis of gout. Meanwhile, the excessive production

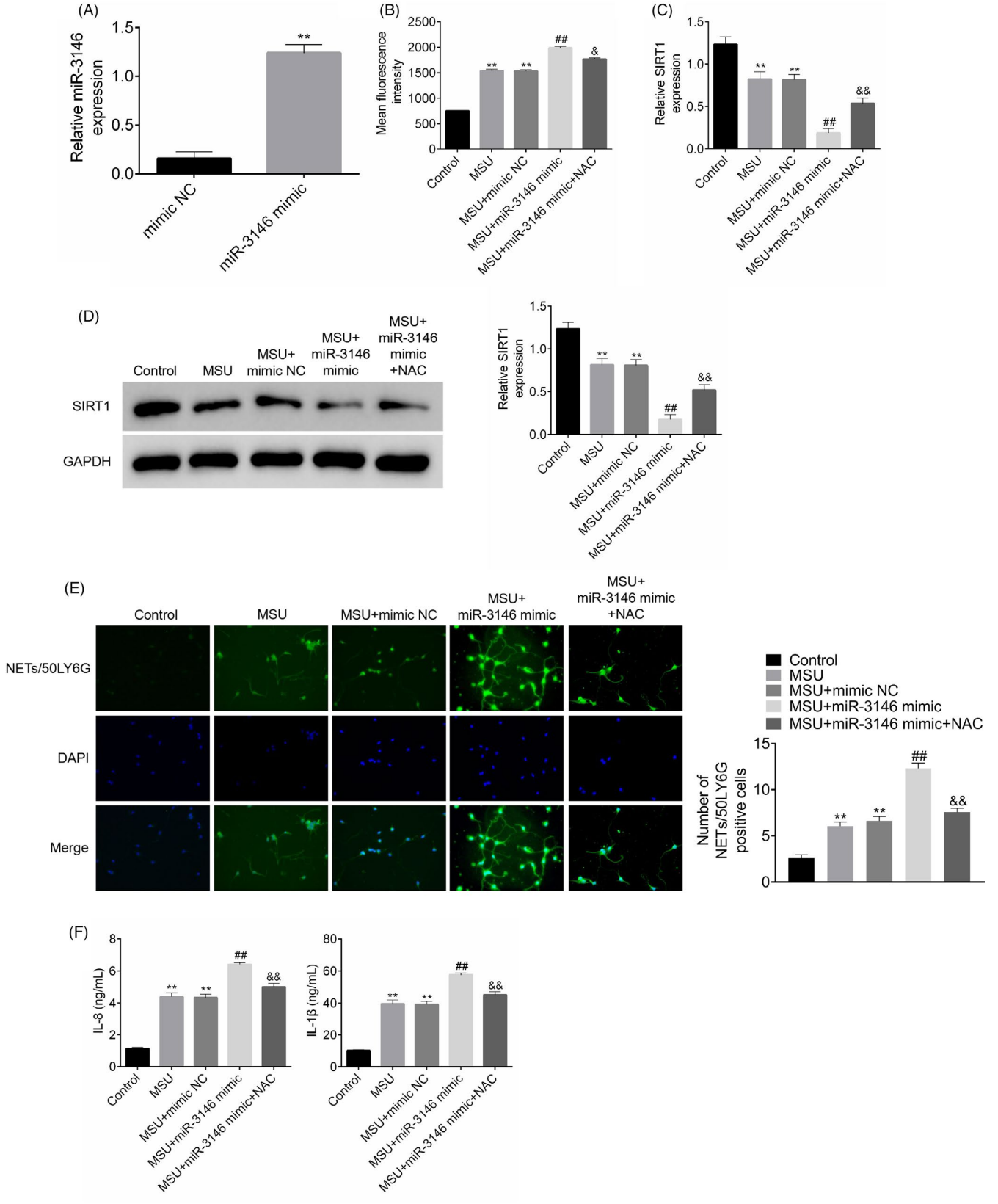

FIGURE 4 MSU crystals trigger NETosis via oxidative stress by regulating miR-3146. The expression of miR-3146 (A), ROS production (B), the mRNA and protein levels of SIRT1 (C, D), NETs formation (E), and the levels of IL-8 and IL-1β (F) in human neutrophils stimulated with MSU crystals or NAC following transfection with miR-3146 mimic. Data from at least three independent experiments ($n = 3$) were expressed as mean ± SD. $^{**}p < 0.01$ versus Control group; $^{\#\#}p < 0.01$ versus MSU + mimic NC group; $^{\&}p < 0.05$, $^{\&\&}p < 0.01$ versus MSU + miR-3146 mimic group

of ROS was also observed in patients with gout compared to the healthy subjects (Figure 1D). Compared to the healthy controls, the mRNA and protein levels of neutrophil SIRT1 were signally decreased in these patients with gout (Figure 1E,F). Furthermore, gout patients showed higher serum levels of proinflammatory cytokines IL-8 and IL-1β compared to the healthy individuals (Figure 1G).

3.2 | Neutrophil miR-3146 and ROS production are increased in response to MSU crystals

We then analyzed the association between miR-3146 and NETosis in gouty arthritis using MSU-induced human neutrophils as cell model. Our data showed that miR-3146 was significantly upregulated in human neutrophils stimulated with MSU crystals (Figure 2A). The addition of MSU crystals efficiently induced NET formation of human neutrophils (Figure 2B,C). As presented in Figure 2D, a higher amount of ROS was produced by human neutrophils subjected to MSU exposure compared to the controls. Moreover, the stimulation of MSU crystals resulted in a decrease of SIRT1 mRNA and protein levels in human neutrophils (Figure 2E,F). Additionally, MSU crystals stimulation led to a higher level of IL-8 and IL-1β in neutrophils (Figure 2G).

3.3 | miR-3146 directly targets SIRT1 in neutrophils

miRNAs are known to function by inhibiting the expression of their target genes. According to the Targetscan analysis results, miR-3146 harbored putative binding sites for SIRT1 (Figure 3A). We further verified the interaction between miR-3146 and SIRT1 using luciferase reporter assay. The results showed that miR-3146 mimic significantly inhibited luciferase activity of SIRT1 WT 3′-UTR, while the luciferase activity of the mutant group was not affected (Figure 3B). miR-3146 overexpression led to SIRT1 downregulation at mRNA and protein levels, while miR-3146 inhibition led to an opposite effect (Figure 3C,D).

3.4 | MSU crystals trigger NETosis via oxidative stress by regulating miR-3146

To further verify whether miR-3146 was implicated in the process of NETosis, miR-3146 expression was overexpressed in human neutrophils via the transfected with miR-3146 mimic. The transfection efficiency was confirmed by qRT-PCR (Figure 4A). Besides, miR-3146 overexpression aggravated ROS excessive generation (Figure 4B), SIRT1 downregulation (Figure 4C,D), NETs formation (Figure 4E), and IL-8 and IL-1β overproduction (Figure 4F) induced by MSU crystals. However, treatment with ROS scavenger NAC in human neutrophils effectively abrogated these effects of miR-3146 overexpression.

3.5 | miR-3146 aggravates gout progression via inducing NETs formation

To ascertain the effects of miR-3146 in gout in vivo, a rat model of acute gouty arthritis was established by injecting MSU crystals into the articular cavity. Compared with the sham-operated group, rats with gout maintained arthritis status (Figure 5A) and exhibited serious swelling (Figure 5B), whereas treatment with antagomir-3146 significantly decreased the arthritis score and edema. As demonstrated by ELISA test, the levels of IL-8 and IL-1β were significantly higher in the gout group than that in the sham-operated group, while treatment with antagomir-3146 markedly reduced the secretion of proinflammatory cytokines (Figure 5C). MDA content was observably increased, while the levels of SOD and GSH-Px were markedly attenuated in the gout group compared to the sham group. Administration with antagomir-3146 significantly led to an opposite effects (Figure 5D). As shown in Figure 5E, gout rats treated with antagomir-3146 showed mild synovial hyperplasia, inflammation and cartilage erosion as evidenced by hematoxylin/eosin staining. Immunofluorescence confocal microscopy confirmed NETs formation in rats with gout, and the effects were reversed by the injection of antagomir-3146 (Figure 5F).

4 | DISCUSSION

In this study, we found that MSU crystals-induced NET release from neutrophils via increasing miR-3146 expression. Further in vivo assay showed that the inhibition of miR-3146 prevented gout progression in experimental rats. Our results provided a novel insight into the contribution of NETosis to the pathogenesis of gout.

Non-coding RNAs are RNA molecules with no protein-coding potential.[18] miRNAs are a class of small non-coding RNAs that participate in various physiological or pathological processes.[19] miRNAs have been implicated as important regulators in the pathogenesis of human inflammatory arthritic diseases, including rats with gout. For instance, Zhou et al.[20] indicated that miR-488 and miR-920 served as anti-inflammatory regulators through IL-1β downregulation in MSU-induced macrophages. Zhang et al.[21]

FIGURE 5 miR-3146 aggravates gout progression via inducing NETs formation. Swollen joint count (A), arthritis index (B), the serum levels of IL-8 and IL-1β (C), the levels of MDA, SOD and GSH-Px (D), histopathological examination of synovial tissues (E) and NETs formation (F) in sham-operated rats or gout rats injected with or without antagomir-3146. Data from at least three independent experiments ($n = 3$) were expressed as mean ± SD. $^{**}p < 0.01$ versus Sham group; $^{\#}p < 0.05$, $^{\#\#}p < 0.01$ versus gout group

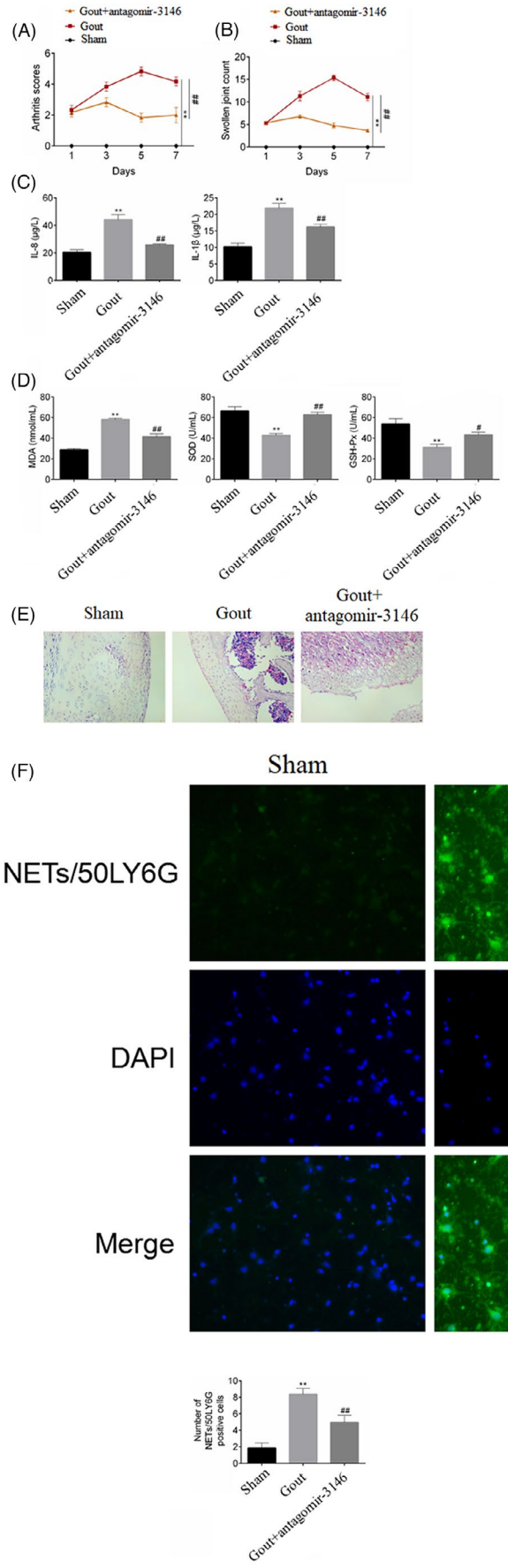
(A)
Gout+antagomir-3146
Gout
Sham
Arthritis scores
Days
(B)
Swollen joint count
(C)
IL-8 (μg/L)
IL-1β (μg/L)
(D)
MDA (nmol/mL)
SOD (U/mL)
GSH-Px (U/mL)
(E)
Sham
Gout
Gout+ antagomir-3146
(F)
NETs/50LY6G
DAPI
Merge
Number of NETs/50LY6G positive cells

implied that miR-146a knockout developed the progression of rats with gout via inhibiting the activation of the NALP3 inflammasome. Herein, upregulated expression of miR-3146 in neutrophils was detected in patients with gout. Additionally, the expression of miR-3146 was higher in human PMNs after exposure to MSU crystals in vitro. Thus, miR-3146 might be a potential therapeutic target for gout.

There is emerging evidence that NETosis is implicated with the occurrence of non-infectious inflammatory diseases.[22,23] Mitroulis et al. demonstrated for the first time that activation of neutrophils is associated with the formation of proinflammatory NETs stimulated with MSU crystals in gout.[24] It has been widely accepted that NETs can play a role in enhancement of the inflammation seen in autoimmune diseases.[25–27] On the contrary, Schauer et al.[28] suggested that aggregated NETs promote the resolution of neutrophilic inflammation by degrading cytokines and chemokines and disrupting neutrophil recruitment and activation. The generation of ROS is required for NETosis by the activation of the nicotinamide adenine dinucleotide phosphate (NADPH) oxidase.[8,29] Indeed, it has recently been shown that MSU crystals induce NETosis in an ROS-dependent manner.[30] In the current research, we showed that the formation of NETs and ROS levels were significantly increased in patients with gout. Additionally, MSU crystals displayed enhanced NETosis and ROS production released by human PMNs, suggesting that MSU crystals triggered NETosis that was dependent on the production of ROS.

To further investigate the molecular mechanism by which miR-3146 contributed to neutrophil-dependent oxidative stress, the potential target genes of miR-3146 were investigated. Here, we found that SIRT1 expression was significantly downregulated in patients with gout and human PMNs following treatment with MSU crystals. As a member of histone deacetylase family, SIRT1 is involved in the regulation of various physiological functions, including glucose and lipid metabolism, oxidative stress injury, inhibition of inflammatory response, and cell proliferation, senescence, and apoptosis through deacetylation.[31] Using bioinformatics, luciferase reporter assays, and miRNA overexpression and knockdown techniques, we identified that miR-3146 could directly target SIRT1 and thereby suppress the expression of SIRT1. Our data further found that excess ROS generation induced by MSU crystals was decreased by miR-3146 overexpression in human PMNs. In contrast, NAC, an ROS scavenger antagonized NETosis and oxidative stress injury induced by miR-3146. Rats with miR-3146 deficiency attenuated MSU crystals-induced synovial inflammation and oxidative damage via dysregulation of NETosis.

In conclusion, we provided the first demonstration that miR-3146 initiated NETosis in an ROS-dependent manner via targeting SIRT1, which ultimately triggered the development of gout. Accordingly, our data suggest that the inhibition of NETosis might be developed as a powerful treatment strategy of gout.

CONFLICT OF INTEREST

The authors have no actual or potential conflicts of interest to declare.

CONSENT TO PARTICIPATE

Informed consent was obtained from all patients and control subjects.

ORCID

Di Yang https://orcid.org/0000-0003-1124-2219

REFERENCES

1. Dalbeth N, Gosling AL, Gaffo A, Abhishek A. Gout. *Lancet*. 2021;397(10287):1843-1855.
2. Cleophas MC, Crisan TO, Joosten LA. Factors modulating the inflammatory response in acute gouty arthritis. *Curr Opin Rheumatol*. 2017;29(2):163-170.
3. Masuda S, Nakazawa D, Shida H, et al. NETosis markers: quest for specific, objective, and quantitative markers. *Clin Chim Acta*. 2016;459:89-93.
4. Sørensen OE, Borregaard N. Neutrophil extracellular traps – the dark side of neutrophils. *J Clin Invest*. 2016;126(5):1612-1620.
5. Desai J, Steiger S, Anders HJ. Molecular pathophysiology of gout. *Trends Mol Med*. 2017;23(8):756-768.
6. Zamudio-Cuevas Y, Hernández-Díaz C, Pineda C, et al. Molecular basis of oxidative stress in gouty arthropathy. *Clin Rheumatol*. 2015;34(10):1667-1672.
7. Liao P, He YI, Yang F, et al. Polydatin effectively attenuates disease activity in lupus-prone mouse models by blocking ROS-mediated NET formation. *Arthritis Res Ther*. 2018;20:254.
8. Vorobjeva NV, Chernyak BV. NETosis: molecular mechanisms, role in physiology and pathology. *Biochemistry (Mosc)*. 2020;85(10):1178-1190.
9. Wang Z, Liu Y. Predicting functional microRNA-mRNA interactions. *Methods Mol Biol*. 2017;1580:117-126.
10. Li X, Pan Y, Li W, Guan P, You C. The role of noncoding RNAs in gout. *Endocrinology*. 2020;161(11):bqaa165.
11. Xu Y-T, Leng Y-R, Liu M-M, et al. MicroRNA and long noncoding RNA involvement in gout and prospects for treatment. *Int Immunopharmacol*. 2020;87:106842.
12. Liu P, Chen Y, Wang B, Wang Z, Li C, Wang Y. Expression of microRNAs in the plasma of patients with acute gouty arthritis and the effects of colchicine and etoricoxib on the differential expression of microRNAs. *Arch Med Sci*. 2019;15(4):1047-1055.
13. Hamburger M, Baraf HSB, Adamson TC, et al. 2011 recommendations for the diagnosis and management of gout and hyperuricemia. *Phys Sportsmed*. 2011;39(4):98-123.
14. Najmeh S, Cools-Lartigue J, Giannias B, Spicer J, Ferri LE. Simplified human neutrophil extracellular traps (NETs) isolation and handling. *J vis Exp*. 2015;98:52687.
15. Caudrillier A, Kessenbrock K, Gilliss BM, et al. Platelets induce neutrophil extracellular traps in transfusion-related acute lung injury. *J Clin Invest*. 2012;122(7):2661-2671.
16. Zhang Y-G, Song Y, Guo X-L, et al. Exosomes derived from oxLDL-stimulated macrophages induce neutrophil extracellular traps to drive atherosclerosis. *Cell Cycle*. 2019;18(20):2674-2684.
17. Gao H, Wang X, Lin C, et al. Exosomal MALAT1 derived from ox-LDL-treated endothelial cells induce neutrophil extracellular traps to aggravate atherosclerosis. *Biol Chem*. 2020;401(3):367-376.
18. Yang JX, Rastetter RH, Wilhelm D. Non-coding RNAs: an introduction. *Adv Exp Med Biol*. 2016;886:13-32.
19. Lu TX, Rothenberg ME. MicroRNA. *J Allergy Clin Immunol*. 2018;141(4):1202-1207.
20. Zhou W, Wang Y, Wu R, He Y, Su Q, Shi G. MicroRNA-488 and -920 regulate the production of proinflammatory cytokines in acute gouty arthritis. *Arthritis Res Ther*. 2017;19(1):203.

21. Zhang Q-B, Qing Y-F, Yin C-C, et al. Mice with miR-146a deficiency develop severe gouty arthritis via dysregulation of TRAF 6, IRAK 1 and NALP3 inflammasome. *Arthritis Res Ther*. 2018;20(1):45.
22. Yousefi S, Stojkov D, Germic N, et al. Untangling "NETosis" from NETs. *Eur J Immunol*. 2019;49(2):221-227.
23. Berthelot JM, Le Goff B, Neel A, Maugars Y, Hamidou M. NETosis: at the crossroads of rheumatoid arthritis, lupus, and vasculitis. *Joint Bone Spine*. 2017;84(3):255-262.
24. Mitroulis I, Kambas K, Chrysanthopoulou A, et al. Neutrophil extracellular trap formation is associated with IL-1beta and autophagy-related signaling in gout. *PLoS One*. 2011;6(12):e29318.
25. Lee KH, Kronbichler A, Park D-Y, et al. Neutrophil extracellular traps (NETs) in autoimmune diseases: a comprehensive review. *Autoimmun Rev*. 2017;16(11):1160-1173.
26. Kumar S, Gupta E, Kaushik S, Jyoti A. Neutrophil extracellular traps: formation and involvement in disease progression. *Iran J Allergy Asthma Immunol*. 2018;17(3):208-220.
27. Mutua V, Gershwin LJ. A review of neutrophil extracellular traps (NETs) in disease: potential anti-NETs therapeutics. *Clin Rev Allergy Immunol*. 2021;61(2):194-211.
28. Schauer C, Janko C, Munoz LE, et al. Aggregated neutrophil extracellular traps limit inflammation by degrading cytokines and chemokines. *Nat Med*. 2014;20(5):511-517.
29. Azzouz D, Khan MA, Palaniyar N. ROS induces NETosis by oxidizing DNA and initiating DNA repair. *Cell Death Discov*. 2021;7(1):113.
30. Schorn C, Janko C, Krenn V, et al. Bonding the foe – NETting neutrophils immobilize the pro-inflammatory monosodium urate crystals. *Front Immunol*. 2012;3:376.
31. Chen YE, Zhou F, Liu H, et al. SIRT1, a promising regulator of bone homeostasis. *Life Sci*. 2021;269:119041.

SUPPORTING INFORMATION

Additional supporting information may be found in the online version of the article at the publisher's website.

How to cite this article: Shan L, Yang D, Feng F, Zhu D, Li X. miR-3146 induces neutrophil extracellular traps to aggravate gout flare. *J Clin Lab Anal*. 2021;35:e24032. https://doi.org/10.1002/jcla.24032